Z. Angew. Math. Phys. (2019) 70:66

0044-2275/19/020001-19
published online March 29, 2019
https://doi.org/10.1007/s00033-019-1111-5

Zeitschrift für angewandte Mathematik und Physik ZAMP

Scattering of transverse surface waves by a piezoelectric fiber in a piezoelectric half-space with exponentially varying electromechanical properties

A. Ghafarollahi and H. M. Shodja

Abstract. In the present work, an analytical solution is presented for the scattering of transverse surface waves by a homogeneous piezoelectric fiber contained in a functionally graded piezoelectric half-space with exponential variation. The boundary value problem of interest is solved by constructing an appropriate set of multipole functions which satisfy: (a) the electromechanical field equations in the half-space, (b) the boundary conditions along its free surface, and (c) the far-filed radiation conditions. It is shown that the simple poles of these functions are related to the roots of the pertinent dispersion relation. For the case of electrically short condition along the free surface of the inhomogeneous half-space, the analytical expressions for the scattered electromechanical fields are derived. In the given numerical examples, the effects of such parameters as the frequency, the distance of the fiber to the substrate's free surface, and the coefficient in the exponent, indicating the variation of the electromechanical properties of the substrate on the scattered fields are addressed in detail. It is seen that these physical parameters have considerable effect on the dynamic response of the medium.

Mathematics Subject Classification. 74J15, 74J20, 82D20.

Keywords. Transverse surface waves, Exponentially graded piezoelectric half-space, Piezoelectric scatterer, Multipole expansion.

1. Introduction

The problem of transverse surface wave propagation through piezoelectric materials or layered structures has received significant attention due to its diverse engineering applications such as surface acoustic wave (SAW) sensors, filters, and delay lines [1]. Special attention has been paid to the propagation of transverse surface waves in typical SAW devices consisting of a piezoelectric layer overlying an elastic substrate or vice versa [2].

Functionally graded piezoelectric materials (FGPMs) are a generation of multifunctional media and play an important role in innovative technological developments. Piezoelectric materials/piezocomposites, due to their electromechanical coupling, have certain advantages over purely elastic materials/composites. FGPMs are designated as graded since their macroscopic properties such as elastic, piezoelectric, and dielectric constants and mass density vary gradually and continuously with the spatial coordinates. This class of smart materials exhibits certain desired functionality features over homogeneous piezoelectric media and has progressively found more applications in industry in recent years. For instance, FGPMs are manufactured and widely used as substrate in SAW devices to improve their efficiency and resolve not only the residual stress problem encountered in layered structures but also the penetration depth issue observed in the homogeneous piezoelectric substrate [3].

The dynamic stress response of media made of FGPMs to elastic waves, especially those containing such defects as cracks and holes, is of particular interest. Du et al. [4] investigated Love waves propagation in a FGPM layer bonded to a semi-infinite homogeneous solid. Qian et al. [5] studied the propagation behavior of Love waves in a homogenous piezoelectric half-space carrying a functionally graded material

Birkhäuser

layer of finite thickness. Eskandari and Shodja [6] investigated the features of Love waves in a FGPM half-space with quadratically varying electromechanical properties. The problem of transverse surface wave propagation in a FGPM substrate with exponentially varying electromechanical properties was studied in the absence of any defect or inhomogeneity by Qian et al. [3]. Recently, Shodja et al. [7] obtained and examined the dispersion relations for the propagation problem of shear horizontal surface acoustic waves in a functionally graded magneto-electro-elastic half-space.

Using the wave function expansion method and the image technique, Fang et al. [8] presented an analytical solution for the scattering problem of shear waves by a circular cavity in a semi-infinite functionally graded piezoelectric material. Fang et al. [9] studied the scattering of electro-elastic waves by two subsurface cavities in a FGPM layer bonded to a homogeneous piezoelectric material. But, to date, the scattering problem of transverse surface waves by a piezoelectric fiber embedded in a functionally graded piezoelectric half-space with exponential variation has not been studied yet. The treatment of this problem is the focus of the current paper. In order to present the scattered electromechanical fields, the multipole expansion method has been used. This method has already been successfully utilized to study the scattering problem of SH-waves by a circular cavity, nano-fiber, and elliptic cavity/crack [10–12].

The paper is organized as follows. In Sect. 2, the problem statement is described and the governing electromechanical field equations are presented. Section 3 is devoted to the formulations of anti-plane scattering of transverse surface waves by a piezoelectric fiber which is located near the free surface of a FGPM half-space with perfect interface—the free surface is assumed to be electrically short. The pertinent electromechanical conditions needed for the well posedness of the proposed problem are presented in this section as well. The exact analytical expressions for the scattered electromechanical fields are derived. Several descriptive examples are provided in Sect. 4. The conclusion is given in Sect. 5.

2. Problem statement and the governing equations

Consider a transversely isotropic functionally graded piezoelectric material (FGPM) half-space, designated as region 1 ($\Omega \equiv 1$), containing a cylindrical piezoelectric fiber of radius a, designated as region 2 ($\Omega \equiv 2$). The origin of the Cartesian coordinates (x, y, z) is set on the surface of the FGPM half-space in such way that the z-axis is directed along the poling direction perpendicular to the xy-plane and the x-axis points down into the substrate and passes through the center of the fiber. A polar coordinate system (r, θ) with origin at the center of the fiber is also considered. The fiber is perfectly bonded to the inhomogeneous substrate at a depth of h beneath its surface, $x = 0$ as depicted in Fig. 1. A time-harmonic transverse surface wave propagating in the positive y-direction is incident upon the fiber.

In the absence of body forces and free charges, the equations of motion and charge equation of electro-statics for a piezoelectric linearly elastic material with varying electromechanical properties are, respectively, given by:

$$\sigma_{ij,j} = \rho(\boldsymbol{x})\ddot{u}_i, \;\; i = 1, 2, 3, \tag{1a}$$

$$D_{j,j} = 0, \tag{1b}$$

and the pertinent constitutive equations are:

$$\begin{Bmatrix} \sigma_{xx} \\ \sigma_{yy} \\ \sigma_{zz} \\ \sigma_{yz} \\ \sigma_{zx} \\ \sigma_{xy} \end{Bmatrix} = \begin{bmatrix} C_{11}(\boldsymbol{x}) & C_{12}(\boldsymbol{x}) & C_{13}(\boldsymbol{x}) & 0 & 0 & 0 \\ C_{12}(\boldsymbol{x}) & C_{11}(\boldsymbol{x}) & C_{13}(\boldsymbol{x}) & 0 & 0 & 0 \\ C_{13}(\boldsymbol{x}) & C_{13}(\boldsymbol{x}) & C_{33}(\boldsymbol{x}) & 0 & 0 & 0 \\ 0 & 0 & 0 & C_{44}(\boldsymbol{x}) & 0 & 0 \\ 0 & 0 & 0 & 0 & C_{44}(\boldsymbol{x}) & 0 \\ 0 & 0 & 0 & 0 & 0 & \frac{1}{2}\left(C_{11}(\boldsymbol{x}) - C_{12}(\boldsymbol{x})\right) \end{bmatrix} \begin{Bmatrix} \varepsilon_{xx} \\ \varepsilon_{yy} \\ \varepsilon_{zz} \\ 2\varepsilon_{yz} \\ 2\varepsilon_{zx} \\ 2\varepsilon_{xy} \end{Bmatrix}$$

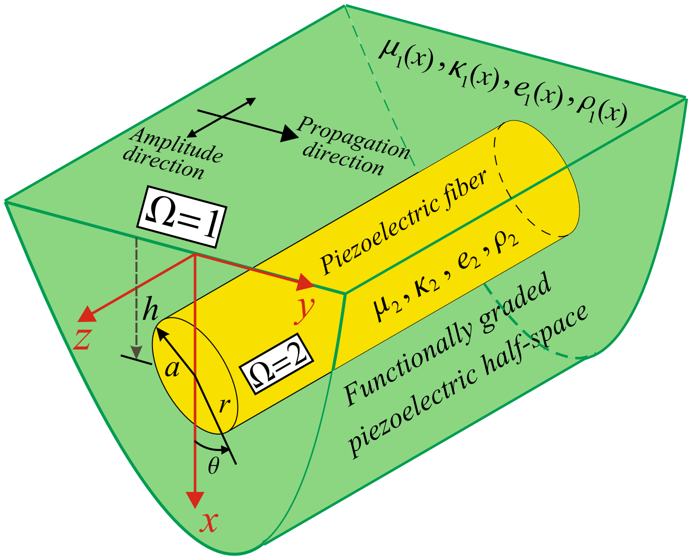

FIG. 1. A homogeneous piezoelectric fiber surrounded by an exponentially graded piezoelectric substrate incident upon by transverse surface waves

$$
+\begin{bmatrix} 0 & 0 & e_{31}(\boldsymbol{x}) \\ 0 & 0 & e_{31}(\boldsymbol{x}) \\ 0 & 0 & e_{33}(\boldsymbol{x}) \\ 0 & e_{15}(\boldsymbol{x}) & 0 \\ e_{15}(\boldsymbol{x}) & 0 & 0 \\ 0 & 0 & 0 \end{bmatrix} \begin{Bmatrix} \phi_{,x} \\ \phi_{,y} \\ \phi_{,z} \end{Bmatrix} \tag{2a}
$$

$$
\begin{Bmatrix} D_x \\ D_y \\ D_z \end{Bmatrix} = \begin{bmatrix} 0 & 0 & 0 & 0 & e_{15}(\boldsymbol{x}) & 0 \\ 0 & 0 & 0 & e_{15}(\boldsymbol{x}) & 0 & 0 \\ e_{31}(\boldsymbol{x}) & e_{31}(\boldsymbol{x}) & e_{33}(\boldsymbol{x}) & 0 & 0 & 0 \end{bmatrix} \begin{Bmatrix} \varepsilon_{xx} \\ \varepsilon_{yy} \\ \varepsilon_{zz} \\ 2\varepsilon_{yz} \\ 2\varepsilon_{zx} \\ 2\varepsilon_{xy} \end{Bmatrix}
$$

$$
-\begin{bmatrix} \kappa_{11}(\boldsymbol{x}) & 0 & 0 \\ 0 & \kappa_{11}(\boldsymbol{x}) & 0 \\ 0 & 0 & \kappa_{33}(\boldsymbol{x}) \end{bmatrix} \begin{Bmatrix} \phi_{,x} \\ \phi_{,y} \\ \phi_{,z} \end{Bmatrix} \tag{2b}
$$

where

$$
\varepsilon_{ij} = \frac{1}{2}\left(u_{i,j} + u_{j,i}\right). \tag{3}
$$

In the above equations, $\boldsymbol{u}$ and $\boldsymbol{D}$ are the mechanical and electrical displacement vectors, respectively. $\boldsymbol{\sigma}$ and $\boldsymbol{\varepsilon}$ are the stress and strain tensors, respectively. ϕ denotes the electric potential function, ρ is the mass density, and $\ddot{\boldsymbol{u}}$ is the acceleration vector. $\boldsymbol{C}(\boldsymbol{x})$, $\boldsymbol{e}(\boldsymbol{x})$, and $\boldsymbol{\kappa}(\boldsymbol{x})$ are the elastic, piezoelectric, and dielectric moduli tensors, respectively. Einsteins summation convention on repeated indices holds.
Further discussion in this section is restricted to anti-plane problems, so that the mechanical displacement field and the electric potential function have the following forms:

$$
\begin{aligned} &u_x = u_y = 0, \quad u_z = u_z(x, y, t), \\ &\phi = \phi(x, y, t). \end{aligned} \tag{4}
$$

By utilization of Eqs. (2)–(4), and assuming that the electromechanical properties are only a function of the coordinate x, it can be shown that Eqs. (1a) and (1b) reduce to [3]:

$$\begin{aligned}
&\frac{\partial \mu(x)}{\partial x}\frac{\partial u_z}{\partial x} + \mu(x)\nabla^2 u_z + \frac{\partial e(x)}{\partial x}\frac{\partial \phi}{\partial x} + e(x)\nabla^2\phi = \rho(x)\ddot{u}_z,\\
&\frac{\partial e(x)}{\partial x}\frac{\partial u_z}{\partial x} + e(x)\nabla^2 u_z - \frac{\partial \kappa(x)}{\partial x}\frac{\partial \phi}{\partial x} - \kappa(x)\nabla^2\phi = 0,
\end{aligned} \tag{5}$$

respectively, where for brevity $\mu(x) \equiv C_{44}(x)$, $e(x) \equiv e_{15}(x)$, and $\kappa(x) \equiv \kappa_{11}(x)$. Moreover, utilizing Eqs. (2)–(4) the nonzero components of the stress and electric displacement fields are obtained as:

$$\sigma_{xz} = \mu(x)\frac{\partial u_z}{\partial x} + e(x)\frac{\partial \phi}{\partial x}, \tag{6a}$$

$$\sigma_{yz} = \mu(x)\frac{\partial u_z}{\partial y} + e(x)\frac{\partial \phi}{\partial y}, \tag{6b}$$

$$D_x = e(x)\frac{\partial u_z}{\partial x} - \kappa(x)\frac{\partial \phi}{\partial x}, \tag{6c}$$

$$D_y = e(x)\frac{\partial u_z}{\partial y} - \kappa(x)\frac{\partial \phi}{\partial y}, \tag{6d}$$

The electromechanical field equations and the constitutive relations for both domains are similar except, the electromechanical properties of the half-space are variable, whereas those of the fiber are constant. Let $\mu_1(x)$, $e_1(x)$, and $\kappa_1(x)$ denote the electromechanical properties of the inhomogeneous medium, while those of the homogeneous piezoelectric fiber are denoted by μ_2, e_2, and κ_2. Moreover, $\rho_1(x)$ and ρ_2 are the mass densities of the FGPM half-space and the fiber, respectively. Here, it is assumed that all the electromechanical properties pertinent to the inhomogeneous functionally graded piezoelectric domain, $\Omega = 1$ vary exponentially with the coordinate x as:

$$\mu_1(x) = \mu_1^0\, e^{\alpha x},\ e_1(x) = e_1^0\, e^{\alpha x},\ \kappa_1(x) = \kappa_1^0\, e^{\alpha x},\ \rho_1(x) = \rho_1^0\, e^{\alpha x}, \tag{7}$$

where μ_1^0, e_1^0, κ_1^0, and ρ_1^0 are the values of $\mu_1(x)$, $e_1(x)$, $\kappa_1(x)$, and $\rho_1(x)$ at the surface as $x \to 0^+$, respectively, and α is a constant coefficient in the exponent, affecting the profile of the material gradient along the coordinate x. It is worth mentioning that the exponentially varying electromechanical properties for the half-space have been previously employed in several studies (e.g., [3–5,8,9]). As it will be shown in Sect. 3.1, for the existence of the transverse surface waves in the FGPM half-space, the condition $\alpha < 0$ must hold. It should also be noted that associated with the transverse surface waves of interest, the incident displacement and electric potential fields decay rapidly with depth. Hence, the presence of the fiber is meaningful when it is placed near the free surface. In Sect. 3, it is readily revealed that the velocity of the surface shear waves in the matrix depends on the properties of the free surface, i.e., μ_1^0, e_1^0, κ_1^0, and ρ_1^0. Thus, the values of the properties at $x \to \infty$ are of no great concern.

3. Formulations and the treatment using multipole expansion

As described in Sect. 2, suppose a time-harmonic transverse surface wave propagating with frequency ω in the positive y-direction is incident upon a piezoelectric fiber which is embedded in a FGPM half-space as shown in Fig. 1. The total displacement field and the total electric potential within the domains $\Omega = 1, 2$ represented, respectively, by $\boldsymbol{u}^{(\Omega)} = u_z^{(\Omega)}\boldsymbol{e}_z$ and $\phi^{(\Omega)}$, where $\boldsymbol{e}_z$ is the base vector along the z-axis may be expressed as:

$$\boldsymbol{u}(x,y,t) = \begin{cases} \boldsymbol{u}^{\mathrm{i}(1)}(x,y,t) + \boldsymbol{u}^{\mathrm{s}(1)}(x,y,t), & x \geq 0\,,\ r > a,\\ \boldsymbol{u}^{\mathrm{r}(2)}(x,y,t), & r < a, \end{cases} \tag{8}$$

$$\phi(x,y,t)=\begin{cases}\phi^{\mathrm{i}(1)}(x,y,t)+\phi^{\mathrm{s}(1)}(x,y,t), & x\geq 0\,,\, r>a,\\ \phi^{\mathrm{r}(2)}(x,y,t), & r<a,\end{cases} \tag{9}$$

In the above equation and the remainder of this paper, the superscripts "i", "s", and "r" over a field quantity indicate that the quantity corresponds to the incident, scattered, and refracted wave fields, respectively. The scattered fields, $u_z^{\mathrm{s}(1)}$ and $\phi^{\mathrm{s}(1)}$, are induced within the inhomogeneous region, $\Omega=1$ due to the presence of the piezoelectric fiber. Utilizing Eqs. (5) and (7)–(9) the coupled electromechanical governing differential equations pertinent to the exponentially graded piezoelectric substrate become:

$$\begin{aligned}&\mu_1^0\left(\nabla^2+\alpha\frac{\partial}{\partial x}\right)\left\{u_z^{\mathrm{i}(1)}+u_z^{\mathrm{s}(1)}\right\}+e_1^0\left(\nabla^2+\alpha\frac{\partial}{\partial x}\right)\left\{\phi^{\mathrm{i}(1)}+\phi^{\mathrm{s}(1)}\right\}=\rho_1^0\left\{\ddot{u}_z^{\mathrm{i}(1)}+\ddot{u}_z^{\mathrm{s}(1)}\right\},\\ &e_1^0\left(\nabla^2+\alpha\frac{\partial}{\partial x}\right)\left\{u_z^{\mathrm{i}(1)}+u_z^{\mathrm{s}(1)}\right\}-\kappa_1^0\left(\nabla^2+\alpha\frac{\partial}{\partial x}\right)\left\{\phi^{\mathrm{i}(1)}+\phi^{\mathrm{s}(1)}\right\}=0.\end{aligned} \tag{10}$$

With the aids of Eqs. (5), (8), and (9), the coupled electromechanical field equations for the displacement field, $u_z^{\mathrm{r}(2)}(x,y,t)$, and the electric potential field, $\phi^{\mathrm{r}(2)}(x,y,t)$ within the piezoelectric fiber take on the following forms:

$$\begin{aligned}&\mu_2\nabla^2u_z^{\mathrm{r}(2)}+e_2\nabla^2\phi^{\mathrm{r}(2)}=\rho_2\ddot{u}_z^{\mathrm{r}(2)},\\ &e_2\nabla^2u_z^{\mathrm{r}(2)}-\kappa_2\nabla^2\phi^{\mathrm{r}(2)}=0,\end{aligned} \tag{11}$$

In order to solve the coupled system of partial differential equations, (10) and (11), the following mixed potential functions are introduced:

$$\begin{aligned}&\psi^{\mathrm{i}(1)}=\phi^{\mathrm{i}(1)}-\frac{e_1^0}{\kappa_1^0}u_z^{\mathrm{i}(1)},\ \psi^{\mathrm{s}(1)}=\phi^{\mathrm{s}(1)}-\frac{e_1^0}{\kappa_1^0}u_z^{\mathrm{s}(1)},\\ &\psi^{\mathrm{r}(2)}=\phi^{\mathrm{r}(2)}-\frac{e_2}{\kappa_2}u_z^{\mathrm{r}(2)},\end{aligned} \tag{12}$$

By substituting Eq. $(12)_1$ into Eq. (10), and Eq. $(12)_2$ into Eq. (11) and, moreover, assuming time-harmonic solutions $\chi(x,y,t)=\tilde{\chi}(x,y)e^{-i\omega t}$ in which χ may represent any of the field variables, the field equations are decoupled as:

$$\begin{aligned}&\left(\nabla^2+\alpha\frac{\partial}{\partial x}+k_1^2\right)\left\{u_z^{\mathrm{i}(1)}+u_z^{\mathrm{s}(1)}\right\}=0,\\ &\left(\nabla^2+\alpha\frac{\partial}{\partial x}\right)\left\{\psi^{\mathrm{i}(1)}+\psi^{\mathrm{s}(1)}\right\}=0,\\ &\left(\nabla^2+k_2^2\right)u_z^{\mathrm{r}(2)}=0,\\ &\nabla^2\psi^{\mathrm{r}(2)}=0.\end{aligned} \tag{13}$$

For convenience, in the above equations and in the subsequent developments, the symbol "∼" over the field quantities is omitted. $k_\Omega=\omega/c_{\mathrm{sh}}^{(\Omega)}$, $\Omega=1,2$ denotes the wave number pertinent to the region Ω, in which $c_{\mathrm{sh}}^{(\Omega)}$ is the propagation velocity of shear waves within the corresponding medium:

$$c_{\mathrm{sh}}^{(1)}=\sqrt{\frac{p_1^0}{\rho_1^0}}, \tag{14}$$

$$c_{\mathrm{sh}}^{(2)}=\sqrt{\frac{p_2}{\rho_2}}, \tag{15}$$

where $p_1^0=\mu_1^0+{e_1^0}^2/\kappa_1^0$ and $p_2=\mu_2+e_2^2/\kappa_2$ are the equivalent shear modulus of the inhomogeneous substrate and the homogeneous piezoelectric fiber, respectively.

3.1. Dispersion relation

Assume that the solutions to Eqs. (13)$_1$ and (13)$_2$ pertinent to the incident displacement and electric potential fields can be expressed as $u_z^{\mathrm{i}(1)}(x,y) = f^{(1)}(x)\exp[i\,k\,y]$ and $\psi^{\mathrm{i}(1)}(x,y) = g^{(1)}(x)\exp[i\,k\,y]$, respectively, in which $k = \omega/c$ denotes the wave number and c is the phase velocity of the transverse surface wave. The boundary conditions associated with the incident wave fields are:

(1) The traction free condition at $x = 0$,

$$\sigma_{xz}^{\mathrm{i}(1)}(0,y) = 0. \tag{16}$$

(2) The electrically short condition at $x = 0$,

$$\phi^{\mathrm{i}(1)}(0,y) = 0. \tag{17}$$

(3) The attenuation conditions as $x \to \infty$,

$$u_z^{\mathrm{i}(1)}, \phi^{\mathrm{i}(1)} \to 0, \text{ as } x \to \infty. \tag{18}$$

Substituting the assumed mechanical displacement and electric potential fields into Eqs. (13)$_1$ and (13)$_2$, yields the following expressions for $f^{(1)}(x)$ and $g^{(1)}(x)$:

$$f^{(1)}(x) = A_1\, e^{-\beta(k)\,x}, \tag{19}$$

$$g^{(1)}(x) = A_2\, e^{-\gamma(k)\,x}, \tag{20}$$

where the attenuation conditions (18) have been used and, moreover, $\beta(k) > 0$ and $\gamma(k) > 0$ are defined as:

$$\begin{aligned} \beta(k) &= \frac{\alpha}{2} + \sqrt{\frac{\alpha^2}{4} + k^2\left(1 - \frac{c^2}{c_{\mathrm{sh}}^{(1)\,2}}\right)}, \\ \gamma(k) &= \frac{\alpha}{2} + \sqrt{\frac{\alpha^2}{4} + k^2}. \end{aligned} \tag{21}$$

The unknown coefficients A_1 and A_2 are determined by satisfying the boundary conditions. It is worth noting that the assumption $\alpha < 0$ gives rise to the condition $c < c_{\mathrm{sh}}$, needed for the existence of the transverse surface waves in the FGPM substrate of interest [3]. Consequently, the incident displacement and electrical potential fields induced within the inhomogeneous domain, $\Omega = 1$ can be written as:

$$u_z^{\mathrm{i}(1)}(x,y) = A_1 e^{-\beta(k)x} \exp[i\,k\,y], \tag{22}$$

$$\phi^{\mathrm{i}(1)}(x,y) = \left(A_2 e^{-\gamma(k)x} + \frac{e_1^0}{\kappa_1^0} A_1 e^{-\beta(k)x}\right) \exp[i\,k\,y]. \tag{23}$$

Theses equations together with Eqs. (6)$_1$, (7)$_1$, (7)$_2$, (16), and (17) lead to the following equations for the unknown coefficients A_1 and A_2:

$$p_1^0 \beta(k) A_1 + e_1^0 \gamma(k) A_2 = 0, \tag{24}$$

$$\frac{e_1^0}{\kappa_1^0} A_1 + A_2 = 0. \tag{25}$$

Solving Eqs. (24) and (25) for the unknown coefficients, the incident displacement and electrical potential fields given by Eqs. (22) and (23) are expressed as:

$$u_z^{\mathrm{i}(1)}(x,y) = u_0 e^{-\beta(k)x} \exp[i\,k\,y], \tag{26}$$

$$\phi^{\mathrm{i}(1)}(x,y) = u_0 \frac{e_1^0}{\kappa_1^0} \left(e^{-\beta(k)x} - e^{-\gamma(k)x}\right) \exp[i\,k\,y], \tag{27}$$

where $u_0 = A_1$ is the amplitude of excitation. It should be mentioned that for nontrivial solution, the determinant of the coefficient matrix must be equal to zero, which leads to the following dispersion relation:

$$\frac{\beta(k)}{\gamma(k)} = \frac{e_1^{0\;2}}{\kappa_1^0 p_1^0}. \tag{28}$$

Clearly, in the absence of the gradient coefficient, i.e., $\alpha = 0$, Eq. (28) leads to the dispersion relation corresponding to transverse surface waves in a homogeneous piezoelectric half-space:

$$\sqrt{1 - \frac{c^2}{c_{\mathrm{sh}}^2}} = \frac{e_1^{0\;2}}{\kappa_1^0 p_1^0}. \tag{29}$$

3.2. Scattered wave fields

Up to this point, the incident mechanical displacement and electrical potential fields associated with the modeled problem have been determined. This section is concerned with the scattered wave fields generated due to the presence of the homogeneous piezoelectric fiber, $\Omega = 2$ surrounded by the inhomogeneous substrate, $\Omega = 1$. The governing equations for the scattered wave fields within the inhomogeneous domain are given by Eqs. $(13)_1$ and $(13)_2$. These equations will take on a more convenient form if we write:

$$\begin{aligned} u_z^{\mathrm{s}(1)}(x, y) &= e^{-\frac{\alpha}{2}x} w^{\mathrm{s}(1)}(x, y), \\ \psi^{\mathrm{s}(1)}(x, y) &= e^{-\frac{\alpha}{2}x} \varphi^{\mathrm{s}(1)}(x, y). \end{aligned} \tag{30}$$

Upon substitution of Eqs. $(30)_1$ and $(30)_2$, respectively, into Eqs. $(13)_1$ and $(13)_2$ we find that $w^{\mathrm{s}(1)}(x, y)$ and $\varphi^{\mathrm{s}(1)}(x, y)$ satisfy the following equations:

$$\left(\nabla^2 + \bar{k}_1^2\right) w^{\mathrm{s}(1)} = 0, \tag{31a}$$

$$\left(\nabla^2 - k_\alpha^2\right) \varphi^{\mathrm{s}(1)} = 0, \tag{31b}$$

where $\bar{k}_1^2 = k_1^2 - \alpha^2/4$ and $k_\alpha = (\alpha^2/4)^{1/2}$. For the sake of simplicity, we assume that $k_1^2 > \alpha^2/4$. For the refracted waves within the fiber the governing equations are expressed by Eqs. $(13)_3$ and $(13)_4$.
The boundary conditions associated with the scattered field along the free surface of the FGPM half-space can be expressed as:

$$\begin{aligned} \sigma_{xz}^{\mathrm{s}(1)} &= 0, \qquad \text{on } x = 0, \\ \phi^{\mathrm{s}(1)} &= 0, \qquad \text{on } x = 0. \end{aligned} \tag{32}$$

Moreover, the continuity of the mechanical displacement, electrical potential field, mechanical traction, and electrical displacement fields, associated with the scattered fields, across the piezoelectric fiber-inhomogeneous matrix interface, respectively, gives:

$$u_z^{\mathrm{s}(1)} + u_z^{\mathrm{i}(1)} - u_z^{\mathrm{r}(2)} = 0, \qquad \text{on } r = a, \tag{33a}$$

$$\phi^{\mathrm{s}(1)} + \phi^{\mathrm{i}(1)} - \phi^{\mathrm{r}(2)} = 0, \qquad \text{on } r = a, \tag{33b}$$

$$\sigma_{rz}^{\mathrm{s}(1)} + \sigma_{rz}^{\mathrm{i}(1)} - \sigma_{rz}^{\mathrm{r}(2)} = 0, \qquad \text{on } r = a, \tag{33c}$$

$$D_r^{\mathrm{s}(1)} + D_r^{\mathrm{i}(1)} - D_r^{\mathrm{r}(2)} = 0, \qquad \text{on } r = a. \tag{33d}$$

Let the functions $u_z^{\mathrm{s}(1)}$ and $\phi^{\mathrm{s}(1)}$ be expressed as:

$$u_z^{\mathrm{s}(1)} = \sum_{\zeta=c,s} \sum_{n=0}^{\infty} \left(a_n^\zeta W_n^{u\zeta} + b_n^\zeta W_n^{\phi\zeta}\right), \tag{34a}$$

$$\phi^{\mathrm{s}(1)} = \sum_{\zeta=c,s}\sum_{n=0}^{\infty}\left(a_n^{\zeta}\Phi_n^{u\zeta} + b_n^{\zeta}\Phi_n^{\phi\zeta}\right), \tag{34b}$$

where

$$\Phi_n^{u\zeta} = \Psi_n^{u\zeta} + \frac{e_1^0}{\kappa_1^0}W_n^{u\zeta}, \tag{35a}$$

$$\Phi_n^{\phi\zeta} = \Psi_n^{\phi\zeta} + \frac{e_1^0}{\kappa_1^0}W_n^{\phi\zeta}, \tag{35b}$$

with

$$W_n^{u\zeta} = e^{-\frac{\alpha}{2}x}\left\{H_n^{(1)}(\bar{k}_1 r)\mathcal{T}_\zeta(n\theta) + F_n^{u\zeta}\right\}, \tag{36a}$$

$$\Psi_n^{u\zeta} = e^{-\frac{\alpha}{2}x}G_n^{u\zeta}, \tag{36b}$$

$$\Psi_n^{\phi\zeta} = e^{-\frac{\alpha}{2}x}\left\{K_n(k_\alpha r)\mathcal{T}_\zeta(n\theta) + G_n^{\phi\zeta}\right\}, \tag{36c}$$

$$W_n^{\phi\zeta} = e^{-\frac{\alpha}{2}x}F_n^{\phi\zeta}. \tag{36d}$$

In the above equations, $H_n^{(1)}$ and K_n are Hankel function of the first kind and modified Bessel function of the second kind, of order n, respectively. a_n^{ζ} and b_n^{ζ} are the unknown constants. $\mathcal{T}_\zeta(n\theta) = \cos(n\theta)$ if $\zeta \equiv c$ and $\mathcal{T}_\zeta(n\theta) = \sin(n\theta)$ if $\zeta \equiv s$. It is required that $F_n^{u\zeta}$ and $F_n^{\phi\zeta}$ satisfy the wave equation (31a), and $G_n^{u\zeta}$ and $G_n^{\phi\zeta}$ satisfy the wave equation (31b). Moreover, the pair $W_n^{u\zeta}$ and $\Phi_n^{u\zeta}$ must satisfy the free surface conditions, Eq. (32). Similarly, the pair $W_n^{\phi\zeta}$ and $\Phi_n^{\phi\zeta}$ must satisfy the free surface conditions, (32). In addition, $F_n^{u\zeta}$, $F_n^{\phi\zeta}$, $G_n^{u\zeta}$, and $G_n^{\phi\zeta}$ must satisfy the radiation conditions at infinity. The functions $H_n^{(1)}(\bar{k}_1 r)\mathcal{T}_\zeta(n\theta)$ and $K_n(k_\alpha r)\mathcal{T}_\zeta(n\theta)$ appeared, respectively, in Eqs. (36a) and (36c) are convenient for handling the boundary conditions on the substrate–fiber interface, $r = a$. They are, however, inconvenient when trying to impose the pertinent boundary conditions along the free surface of the substrate, $x = 0$. To overcome this difficulty, we convert the functions $H_n^{(1)}\left(\bar{k}_1 r\right)\mathcal{T}_\zeta(n\theta)$ and $K_n\left(k_\alpha r\right)\mathcal{T}_\zeta(n\theta)$ from polar coordinates to Cartesian coordinates by employing the following integral representations for $H_n^{(1)}(\bar{k}_1 r)\mathcal{T}_\zeta(n\theta)$ and $K_n(k_\alpha r)\mathcal{T}_\zeta(n\theta)$ [13]:

$$H_n^{(1)}(\bar{k}_1 r)\mathcal{T}_\zeta(n\theta) = \frac{(-1)^n}{\pi\, i}\chi^{\zeta}\int_{-\infty}^{\infty+\pi i} e^{-\bar{k}_1 x\sinh\tau}e^{\bar{k}_1 h\sinh\tau - n\tau}\mathcal{T}_\zeta(\bar{k}_1 y\cosh\tau)\mathrm{d}\tau, \quad x<h, |y|<\infty, \tag{37a}$$

$$K_n(k_\alpha r)\mathcal{T}_\zeta(n\theta) = \frac{(-1)^n}{2}\int_{-\infty}^{\infty} e^{k_\alpha x\cosh\upsilon}e^{-k_\alpha h\cosh\upsilon - n\upsilon}\mathcal{T}_\zeta(k_\alpha y\sinh\upsilon)\mathrm{d}\upsilon, \quad x<h, |y|<\infty, \tag{37b}$$

which can conveniently be used on the substrate's free surface ($x = 0$). In the above relations $\chi^{\zeta} = 1$ if $\zeta \equiv c$ and $\chi^{\zeta} = -1$ if $\zeta \equiv s$. Subsequently, the following integral representations for $F_n^{u\zeta}$, $F_n^{\phi\zeta}$, $G_n^{u\zeta}$, and $G_n^{\phi\zeta}$ are considered:

$$F_n^{u\zeta}(x,y) = \frac{(-1)^n}{\pi\, i}\chi^{\zeta}\int_{-\infty}^{\infty+\pi i} A(\tau)e^{\bar{k}_1 x\sinh\tau}e^{\bar{k}_1 h\sinh\tau - n\tau}\mathcal{T}_\zeta(\bar{k}_1 y\cosh\tau)\mathrm{d}\tau, \quad x>0, \tag{38a}$$

$$G_n^{u\zeta}(x,y) = \frac{(-1)^n}{\pi\, i}\chi^{\zeta}\int_{-\infty}^{\infty+\pi i} B(\tau)e^{-x\Delta(\tau)}e^{\bar{k}_1 h\sinh\tau - n\tau}\mathcal{T}_\zeta(\bar{k}_1 y\cosh\tau)\mathrm{d}\tau, \quad x>0, \tag{38b}$$

$$G_n^{\phi\zeta}(x,y) = \frac{(-1)^n}{2}\int_{-\infty}^{\infty} C(\upsilon)e^{-k_\alpha x\cosh\upsilon}e^{-k_\alpha h\cosh\upsilon - n\upsilon}\mathcal{T}_\zeta(k_\alpha y\sinh\upsilon)\mathrm{d}\upsilon, \quad x>0, \tag{38c}$$

$$F_n^{\phi\zeta}(x,y) = \frac{(-1)^n}{2}\int_{-\infty}^{\infty} D(\upsilon)e^{-x\Gamma(\upsilon)}e^{-k_\alpha h\cosh\upsilon - n\upsilon}\mathcal{T}_\zeta(k_\alpha y\sinh\upsilon)\mathrm{d}\upsilon, \quad x>0. \tag{38d}$$

In the above equations, $A(\tau)$, $B(\tau)$, $C(\upsilon)$, and $D(\upsilon)$ are the unknown functions to be determined through the enforcement of the pertinent boundary conditions along the free surface of the FGP half-space. $F_n^{u\zeta}$ and $G_n^{\phi\zeta}$ satisfy Eqs. (31a) and (31b) automatically for any reasonable choice of $A(\tau)$ and $C(\upsilon)$, respectively. Moreover, $F_n^{\phi\zeta}$ and $G_n^{u\zeta}$ must satisfy Eqs. (31a) and (31b), respectively, which yields:

$$\Delta^2(\tau) = \bar{k}_1^2\cosh^2\tau + k_\alpha^2, \tag{39a}$$

$$\Gamma^2(\upsilon) = k_\alpha^2\sinh^2\upsilon - \bar{k}_1^2. \tag{39b}$$

Depending on the values of $\bar{k}_1$, k_α, and υ, $\Gamma(\upsilon)$ may be real or pure imaginary, whereas $\Delta(\tau)$ is always real. It should be noted that $G_n^{u\zeta}$ and $F_n^{\phi\zeta}$ must be bounded as $x\to\infty$, and thus, $\Delta(\tau)$ and $\Gamma(\upsilon)$ cannot take on negative real values. Moreover, to ensure that the scattered waves propagate away from the free surface, it is required that $\mathrm{Im}[\Gamma(\upsilon)]<0$.

With the aids of Eqs. (32) and (56)–(38), the following expressions for $A(\tau)$, $B(\tau)$, $C(\upsilon)$, and $D(\upsilon)$ are found:

$$A(\tau) = -\frac{\kappa_1^0 p_1^0\left(\alpha + 2\bar{k}_1\sinh\tau\right) - {e_1^0}^2\left(\alpha + 2\Delta(\tau)\right)}{\kappa_1^0 p_1^0\left(\alpha - 2\bar{k}_1\sinh\tau\right) - {e_1^0}^2\left(\alpha + 2\Delta(\tau)\right)}, \tag{40a}$$

$$B(\tau) = \frac{4e_1^0 p_1^0\bar{k}_1\sinh\tau}{\kappa_1^0 p_1^0\left(\alpha - 2\bar{k}_1\sinh\tau\right) - {e_1^0}^2\left(\alpha + 2\Delta(\tau)\right)}, \tag{40b}$$

$$C(\upsilon) = -\frac{{e_1^0}^2\left(\alpha - 2k_\alpha\cosh\upsilon\right) - \kappa_1^0 p_1^0\left(\alpha + 2\Gamma(\upsilon)\right)}{{e_1^0}^2\left(\alpha + 2k_\alpha\cosh\upsilon\right) - \kappa_1^0 p_1^0\left(\alpha + 2\Gamma(\upsilon)\right)}, \tag{40c}$$

$$D(\upsilon) = -\frac{4e_1^0\kappa_1^0 k_\alpha\cosh\upsilon}{{e_1^0}^2\left(\alpha + 2k_\alpha\cosh\upsilon\right) - \kappa_1^0 p_1^0\left(\alpha + 2\Gamma(\upsilon)\right)}. \tag{40d}$$

Now, let

$$\kappa_1^0 p_1^0\left(\alpha - 2\bar{k}_1\sinh\tau\right) - {e_1^0}^2\left(\alpha + 2\Delta(\tau)\right) \equiv H(\bar{k}_1\cosh\tau), \tag{41a}$$

$${e_1^0}^2\left(\alpha + 2k_\alpha\cosh\upsilon\right) - \kappa_1^0 p_1^0\left(\alpha + 2\Gamma(\upsilon)\right) \equiv R(k_\alpha\sinh\upsilon), \tag{41b}$$

where

$$H(\lambda) = \frac{\kappa_1^0 p_1^0}{2}\beta(\lambda) - \frac{{e_1^0}^2}{2}\gamma(\lambda), \tag{42a}$$

$$R(\lambda) = \frac{{e_1^0}^2}{2}\gamma(\lambda) - \frac{\kappa_1^0 p_1^0}{2}\beta(\lambda). \tag{42b}$$

It can be observed that $H(\lambda)=0$ and $R(\lambda)=0$ are identical to the dispersion relation given by Eq. (28). Therefore, $H(\lambda)$ and $R(\lambda)$ have only two zeros, $\pm\lambda_0$, where λ_0 is real and positive. Hence, $H(\bar{k}_1\cosh\tau)$ has two simple poles, $-\tau_0$ and $\tau_0 + \pi i$ on the contour of integration, where $\tau_0 = \cosh^{-1}(\lambda_0/\bar{k}_1)$, Fig. 2a. Similarly, $R(k_\alpha\sinh\upsilon)$ has simple poles $-\upsilon_0$ and υ_0 on the contour of integration, where $\upsilon_0 = \sinh^{-1}(\lambda_0/k_\alpha)$, Fig. 2b.

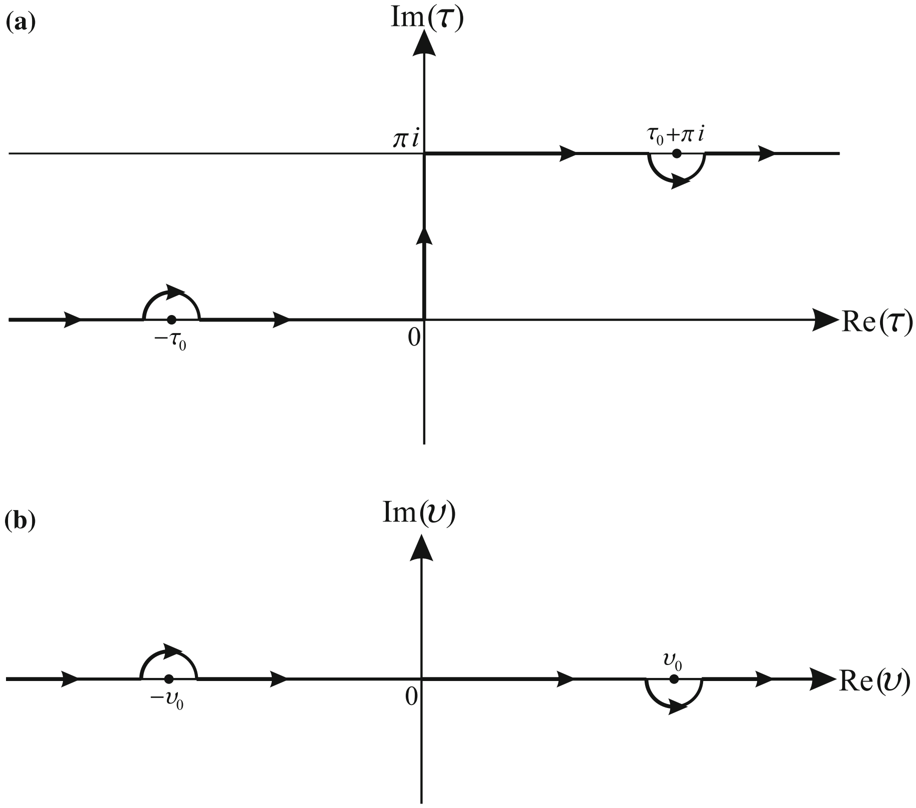

FIG. 2. Contour of integration and the simple poles pertinent to the integral expressions of **a** $F_n^{u\zeta}$ and $G_n^{u\zeta}$, and **b** $G_n^{\phi\zeta}$ and $F_n^{\phi\zeta}$

The refracted waves inside the piezoelectric fiber which satisfy the wave Eqs. $(13)_3$ and $(13)_4$ are standing waves and can be expressed as:

$$u_z^{\mathrm{r}(2)} = \sum_{\zeta=c,s}\sum_{n=0}^{\infty} c_n^{\zeta} J_n(k_2 r)\mathcal{T}_{\zeta}(n\theta),$$
$$\psi^{\mathrm{r}(2)} = \sum_{\zeta=c,s}\sum_{n=0}^{\infty} d_n^{\zeta} r^n \mathcal{T}_{\zeta}(n\theta). \tag{43}$$

Substituting the above relations into Eq. $(12)_2$, the refracted electric potential field within the piezoelectric fiber can be obtained as:

$$\phi^{\mathrm{r}(2)} = \sum_{\zeta=c,s}\sum_{n=0}^{\infty}\left(\frac{e_2}{\kappa_2} c_n^{\zeta} J_n(k_2 r) + d_n^{\zeta} r^n\right)\mathcal{T}_{\zeta}(n\theta). \tag{44}$$

In the above equations, c_n^{ζ} and d_n^{ζ} are the unknown constants and J_n is the Bessel function of the first kind of order n. It remains to determine the coefficients a_n^{ζ}, b_n^{ζ}, c_n^{ζ}, and d_n^{ζ} by imposing the boundary conditions along the homogeneous piezoelectric fiber-inhomogeneous substrate interface, Eqs. (33). To this end, at first, the mechanical displacement and electrical potential fields pertinent to the incident and scattered waves are represented as Fourier series in θ. Thus, $u_z^{\mathrm{i}(1)}$ and $\phi^{\mathrm{i}(1)}$ which are given by Eqs. (26) and (27), respectively, may be written as:

$$
\begin{aligned}
u_z^{\mathrm{i}(1)} &= u_0 e^{-\beta(k)x+ikr\sin\theta} \\
&= u_0 e^{-\beta(k)x} \sum_{\zeta=c,s} \sum_{m=0}^{\infty} \frac{\varepsilon_m}{2} \varsigma^{\zeta} \left\{ J_m(kr) + \chi^{\zeta} J_{-m}(kr) \right\} \mathcal{T}_{\zeta}(m\theta), \qquad (45) \\
\phi^{\mathrm{i}(1)} &= u_0 \frac{e_1^0}{\kappa_1^0} \left(e^{-\beta(k)x} - e^{-\gamma(k)x} \right) e^{ikr\sin\theta} \\
&= u_0 \frac{e_1^0}{\kappa_1^0} \left(e^{-\beta(k)x} - e^{-\gamma(k)x} \right) \sum_{\zeta=c,s} \sum_{m=0}^{\infty} \frac{\varepsilon_m}{2} \varsigma^{\zeta} \left\{ J_m(kr) + \chi^{\zeta} J_{-m}(kr) \right\} \mathcal{T}_{\zeta}(m\theta), \qquad (46)
\end{aligned}
$$

respectively, where $\varsigma^{\zeta} = 1$ if $\zeta = c$ and $\varsigma^{\zeta} = i$ if $\zeta = s$. Furthermore, Eqs. (45) and (46) are reduced to:

$$
u_z^{\mathrm{i}(1)}(r,\theta) = \sum_{\zeta=c,s} \sum_{m=0}^{\infty} (-1)^m \frac{\varepsilon_m}{2} Q_m^{\zeta}(r) \mathcal{T}_{\zeta}(m\theta), \qquad (47a)
$$

$$
\phi^{\mathrm{i}(1)}(r,\theta) = \frac{e_1^0}{\kappa_1^0} \sum_{\zeta=c,s} \sum_{m=0}^{\infty} (-1)^m \frac{\varepsilon_m}{2} \left\{ Q_m^{\zeta}(r) - Z_m^{\zeta}(r) \right\} \mathcal{T}_{\zeta}(m\theta), \qquad (47b)
$$

where

$$
\begin{aligned}
Q_m^{\zeta}(r) &= u_0 e^{-\beta(k)h} \sum_{p=0}^{\infty} (-1)^p \frac{\varepsilon_p}{2} \varsigma^{\zeta} \left\{ I_{m-p}(\beta(k)r) + \chi^{\zeta} I_{-m-p}(\beta(k)r) \right\} \\
&\quad \times \left\{ J_p(kr) + \chi^{\zeta} J_{-p}(kr) \right\}, \qquad (48) \\
Z_m^{\zeta}(r) &= u_0 e^{-\gamma(k)h} \sum_{p=0}^{\infty} (-1)^p \frac{\varepsilon_p}{2} \varsigma^{\zeta} \left\{ I_{m-p}(\gamma(k)r) + \chi^{\zeta} I_{-m-p}(\gamma(k)r) \right\} \\
&\quad \times \left\{ J_p(kr) + \chi^{\zeta} J_{-p}(kr) \right\}. \qquad (49)
\end{aligned}
$$

In the above equations, I_m is the modified Bessel function of the first kind of order m, $\varepsilon_0 = 1$ and $\varepsilon_m = 2$ for $m = 1, 2, 3, \ldots$. In arriving at expressions (47a) and (47b), the following series representation of $e^{-\gamma x}$ for constant γ has been employed:

$$
e^{-\gamma x} = e^{-\gamma h} \sum_{p=0}^{\infty} (-1)^p \frac{\varepsilon_p}{2} \left\{ I_p(\gamma r) + I_{-p}(\gamma r) \right\} \cos(p\theta). \qquad (50)
$$

In a similar way, utilizing the relations:

$$
\begin{aligned}
e^{\bar{k}_1 x \sinh\tau} \mathcal{T}_{\zeta}(\bar{k}_1 y \cosh\tau) &= e^{\bar{k}_1 h \sinh\tau} \sum_{m=0}^{\infty} (-1)^m \frac{\varepsilon_m}{2} \left\{ \chi^{\zeta} e^{-m\tau} + (-1)^m e^{m\tau} \right\} \\
&\quad \times J_m(\bar{k}_1 r) \mathcal{T}_{\zeta}(m\theta), \qquad (51a) \\
e^{-k_\alpha x \cosh\upsilon} \mathcal{T}_{\zeta}(k_\alpha y \sinh\upsilon) &= e^{-k_\alpha h \cosh\upsilon} \sum_{m=0}^{\infty} (-1)^m \frac{\varepsilon_m}{2} \left\{ e^{-m\upsilon} + \chi^{\zeta} e^{m\upsilon} \right\} \\
&\quad \times I_m(k_\alpha r) \mathcal{T}_{\zeta}(m\theta), \qquad (51b)
\end{aligned}
$$

and Eqs. (38) we obtain:

$$
F_n^{u\zeta}(r,\theta) = \sum_{m=0}^{\infty} (-1)^m \frac{\varepsilon_m}{2} f_{mn}^{u\zeta} J_m\left(\bar{k}_1 r\right) \mathcal{T}_{\zeta}(m\theta), \quad 0 < r < b, \qquad (52a)
$$

$$
G_n^{u\zeta}(r,\theta) = \sum_{m=0}^{\infty} (-1)^m \frac{\varepsilon_m}{2} g_{mn}^{u\zeta} I_m(k_\alpha r) \mathcal{T}_{\zeta}(m\theta), \quad 0 < r < b, \qquad (52b)
$$

$$G_n^{\phi\zeta}(r,\theta)=\sum_{m=0}^{\infty}(-1)^m\frac{\varepsilon_m}{2}g_{mn}^{\phi\zeta}I_m\left(k_\alpha r\right)\mathcal{T}_\zeta(m\theta),\quad 0<r<b, \tag{52c}$$

$$F_n^{\phi\zeta}(r,\theta)=\sum_{m=0}^{\infty}(-1)^m\frac{\varepsilon_m}{2}f_{mn}^{\phi\zeta}J_m\left(\bar{k}_1 r\right)\mathcal{T}_\zeta(m\theta),\quad 0<r<b, \tag{52d}$$

where

$$f_{mn}^{u\zeta}=\frac{(-1)^n}{\pi\, i}\chi^\zeta\int_{-\infty}^{\infty+\pi i}A(\tau)e^{2\bar{k}_1 h\sinh\tau}\left\{\chi^\zeta e^{-(m+n)\tau}+(-1)^m e^{(m-n)\tau}\right\}\mathrm{d}\tau, \tag{53a}$$

$$g_{mn}^{u\zeta}=\frac{(-1)^n}{\pi\, i}\chi^\zeta\int_{-\infty}^{\infty}\tilde{B}(\upsilon)e^{-h(\Gamma(\upsilon)+k_\alpha\cosh\upsilon)}\left(\frac{\Gamma(\upsilon)+k_\alpha\sinh\upsilon}{\bar{k}_1}\right)^n$$
$$\times\left\{e^{-m\upsilon}+\chi^\zeta e^{m\upsilon}\right\}\frac{k_\alpha\cosh\upsilon}{\Gamma(\upsilon)}\mathrm{d}\upsilon, \tag{53b}$$

$$g_{mn}^{\phi\zeta}=\frac{(-1)^n}{2}\int_{-\infty}^{\infty}C(\upsilon)e^{-2k_\alpha h\cosh\tau}\left\{e^{-(m+n)\upsilon}+\chi^\zeta e^{(m-n)\upsilon}\right\}\mathrm{d}\upsilon, \tag{53c}$$

$$f_{mn}^{\phi\zeta}=\frac{(-1)^n}{2}\int_{-\infty}^{\infty+\pi i}\tilde{D}(\tau)e^{h(\bar{k}_1\sinh\tau-\Delta(\tau))}\left(\frac{\Delta(\tau)-\bar{k}_1\cosh\tau}{k_\alpha}\right)^n$$
$$\times\left\{\chi^\zeta e^{-m\tau}+(-1)^m e^{m\tau}\right\}\frac{\bar{k}_1\sinh\tau}{\Delta(\tau)}\mathrm{d}\tau, \tag{53d}$$

with

$$\tilde{B}(\upsilon)=\frac{4\,e_1^0\,p_1^0\,\Gamma(\upsilon)}{{e_1^0}^2\left(\alpha+2k_\alpha\cosh\upsilon\right)-\kappa_1^0 p_1^0\left(\alpha+2\Gamma(\upsilon)\right)}, \tag{54}$$

$$\tilde{D}(\tau)=-\frac{4\,e_1^0\,\kappa_1^0\,\Delta(\tau)}{\kappa_1^0 p_1^0\left(\alpha-2\bar{k}_1\sinh\tau\right)-{e_1^0}^2\left(\alpha+2\Delta(\tau)\right)}, \tag{55}$$

It is worth mentioning that in arriving at expressions (52b) and (52d), the change of variable $\bar{k}_1\cosh\tau=k_\alpha\sinh\upsilon$ has been made. Employing Eqs. (56)–(36) along with the expansion relation (50), we find the following expressions for the scattered displacement pertinent to the inhomogeneous half-space:

$$u_z^{\mathrm{s}(1)}=e^{-\frac{\alpha}{2}h}\sum_{\zeta=c,s}\sum_{n=0}^{\infty}\sum_{m=0}^{\infty}(-1)^m\frac{\varepsilon_m}{2}\left(a_n^\zeta\mathcal{F}_{mn}^{u\zeta}(r)+b_n^\zeta\mathcal{F}_{mn}^{\phi\zeta}(r)\right)\mathcal{T}_\zeta(m\theta),$$

$$\phi^{\mathrm{s}(1)}=e^{-\frac{\alpha}{2}h}\sum_{\zeta=c,s}\sum_{n=0}^{\infty}\sum_{m=0}^{\infty}(-1)^m\frac{\varepsilon_m}{2}\left(a_n^\zeta\left\{\mathcal{G}_{mn}^{u\zeta}(r)+\frac{e_1^0}{\kappa_1^0}\mathcal{F}_{mn}^{u\zeta}(r)\right\}\right.$$
$$\left.+b_n^\zeta\left\{\mathcal{G}_{mn}^{\phi\zeta}(r)+\frac{e_1^0}{\kappa_1^0}\mathcal{F}_{mn}^{\phi\zeta}(r)\right\}\right)\mathcal{T}_\zeta(m\theta), \tag{56a}$$

where

$$\mathcal{F}_{mn}^{u\zeta}(r)=(-1)^n\left\{I_{m-n}\left(\frac{\alpha}{2}r\right)+\chi^\zeta I_{-m-n}\left(\frac{\alpha}{2}r\right)\right\}H_n^{(1)}\left(\bar{k}_1 r\right)$$
$$+\sum_{p=0}^{\infty}\frac{\varepsilon_p}{2}f_{pn}^{u\zeta}\left\{I_{m-p}\left(\frac{\alpha}{2}r\right)+\chi^\zeta I_{-m-p}\left(\frac{\alpha}{2}r\right)\right\}J_p\left(\bar{k}_1 r\right), \tag{57a}$$

$$\mathcal{G}^{u\zeta}_{mn}(r)=\sum_{p=0}^{\infty}\frac{\varepsilon_p}{2}g^{u\zeta}_{pn}\left\{I_{m-p}\left(\frac{\alpha}{2}r\right)+\chi^{\zeta}I_{-m-p}\left(\frac{\alpha}{2}r\right)\right\}I_p\left(k_\alpha r\right), \tag{57b}$$

$$\begin{aligned}\mathcal{G}^{\phi\zeta}_{mn}(r)&=(-1)^n\left\{I_{m-n}\left(\frac{\alpha}{2}r\right)+\chi^{\zeta}I_{-m-n}\left(\frac{\alpha}{2}r\right)\right\}K_n\left(k_\alpha r\right)\\&\quad+\sum_{p=0}^{\infty}\frac{\varepsilon_p}{2}g^{\phi\zeta}_{pn}\left\{I_{m-p}\left(\frac{\alpha}{2}r\right)+\chi^{\zeta}I_{-m-p}\left(\frac{\alpha}{2}r\right)\right\}I_p\left(k_\alpha r\right),\end{aligned} \tag{57c}$$

$$\mathcal{F}^{\phi\zeta}_{mn}(r)=\sum_{p=0}^{\infty}\frac{\varepsilon_p}{2}f^{\phi\zeta}_{pn}\left\{I_{m-p}\left(\frac{\alpha}{2}r\right)+\chi^{\zeta}I_{-m-p}\left(\frac{\alpha}{2}r\right)\right\}J_p\left(\bar{k}_1 r\right). \tag{57d}$$

With the aids of Eqs. (6), (3), (7), (47), and (56), the stress components $\sigma^{\mathrm{i}(1)}_{rz}$ and $\sigma^{\mathrm{s}(1)}_{rz}$, and the electric displacement components $D^{\mathrm{i}(1)}_r$ and $D^{\mathrm{s}(1)}_r$ induced, respectively, by the incident and scattered waves within the functionally graded half-space are also obtained:

$$\begin{aligned}\sigma^{\mathrm{i}(1)}_{rz}(r,\theta)&=\mu^0_1e^{\alpha h}\sum_{\zeta=c,s}\sum_{m=0}^{\infty}\frac{\varepsilon_m}{2}\mathbb{Q}^{\zeta}_m(r)\mathcal{T}_\zeta(m\theta)\\&\quad+\frac{{e^0_1}^2}{\kappa^0_1}e^{\alpha h}\sum_{\zeta=c,s}\sum_{m=0}^{\infty}\frac{\varepsilon_m}{2}\left\{\mathbb{Q}^{\zeta}_m(r)-\mathbb{Z}^{\zeta}_m(r)\right\}\mathcal{T}_\zeta(m\theta),\end{aligned} \tag{58a}$$

$$\begin{aligned}\sigma^{\mathrm{s}(1)}_{rz}(r,\theta)&=\mu^0_1e^{\frac{\alpha}{2}h}\sum_{\zeta=c,s}\sum_{n=0}^{\infty}\sum_{m=0}^{\infty}\frac{\varepsilon_m}{2}\left(a^{\zeta}_n\mathbb{F}^{u\zeta}_{mn}(r)+b^{\zeta}_n\mathbb{F}^{\phi\zeta}_{mn}(r)\right)\mathcal{T}_\zeta(m\theta)\\&\quad+e^0_1e^{\frac{\alpha}{2}h}\sum_{\zeta=c,s}\sum_{n=0}^{\infty}\sum_{m=0}^{\infty}\frac{\varepsilon_m}{2}\left(a^{\zeta}_n\left\{\mathbb{G}^{u\zeta}_{mn}(r)+\frac{e^0_1}{\kappa^0_1}\mathbb{F}^{u\zeta}_{mn}(r)\right\}\right.\\&\quad\left.+b^{\zeta}_n\left\{\mathbb{G}^{\phi\zeta}_{mn}(r)+\frac{e^0_1}{\kappa^0_1}\mathbb{F}^{\phi\zeta}_{mn}(r)\right\}\right)\mathcal{T}_\zeta(m\theta),\end{aligned} \tag{58b}$$

$$\begin{aligned}D^{\mathrm{i}(1)}_r(r,\theta)&=e^0_1e^{\alpha h}\sum_{\zeta=c,s}\sum_{m=0}^{\infty}\frac{\varepsilon_m}{2}\mathbb{Q}^{\zeta}_m(r)\mathcal{T}_\zeta(m\theta)\\&\quad-{e^0_1}^2e^{\alpha h}\sum_{\zeta=c,s}\sum_{m=0}^{\infty}\frac{\varepsilon_m}{2}\left\{\mathbb{Q}^{\zeta}_m(r)-\mathbb{Z}^{\zeta}_m(r)\right\}\mathcal{T}_\zeta(m\theta),\end{aligned} \tag{58c}$$

$$\begin{aligned}D^{\mathrm{s}(1)}_r(r,\theta)&=e^0_1e^{\frac{\alpha}{2}h}\sum_{\zeta=c,s}\sum_{n=0}^{\infty}\sum_{m=0}^{\infty}\frac{\varepsilon_m}{2}\left(a^{\zeta}_n\mathbb{F}^{u\zeta}_{mn}(r)+b^{\zeta}_n\mathbb{F}^{\phi\zeta}_{mn}(r)\right)\mathcal{T}_\zeta(m\theta)\\&\quad-\kappa^0_1e^{\frac{\alpha}{2}h}\sum_{\zeta=c,s}\sum_{n=0}^{\infty}\sum_{m=0}^{\infty}\frac{\varepsilon_m}{2}\left(a^{\zeta}_n\left\{\mathbb{G}^{u\zeta}_{mn}(r)+\frac{e^0_1}{\kappa^0_1}\mathbb{F}^{u\zeta}_{mn}(r)\right\}\right.\\&\quad\left.+b^{\zeta}_n\left\{\mathbb{G}^{\phi\zeta}_{mn}(r)+\frac{e^0_1}{\kappa^0_1}\mathbb{F}^{\phi\zeta}_{mn}(r)\right\}\right)\mathcal{T}_\zeta(m\theta),\end{aligned} \tag{58d}$$

in which

$$\mathbb{Q}^{\zeta}_m(r)=\sum_{s=0}^{\infty}\frac{\varepsilon_s}{2}(-1)^s\left\{I_{m-s}(\alpha\,r)+\chi^{\zeta}I_{-m-s}(\alpha\,r)\right\}\frac{\partial\,Q^{\zeta}_s(r)}{\partial\,r}, \tag{59a}$$

$$\mathbb{Z}^{\zeta}_m(r)=\sum_{s=0}^{\infty}\frac{\varepsilon_s}{2}(-1)^s\left\{I_{m-s}(\alpha\,r)+\chi^{\zeta}I_{-m-s}(\alpha\,r)\right\}\frac{\partial\,Z^{\zeta}_s(r)}{\partial\,r}, \tag{59b}$$

$$\mathbb{F}^{u\zeta}_{mn}(r) = \sum_{s=0}^{\infty} \frac{\varepsilon_s}{2}(-1)^s \left\{ I_{m-s}(\alpha\, r) + \chi^\zeta I_{-m-s}(\alpha\, r)\right\} \frac{\partial\, \mathcal{F}^{u\zeta}_{sn}(r)}{\partial\, r}, \tag{59c}$$

$$\mathbb{F}^{\phi\zeta}_{mn}(r) = \sum_{s=0}^{\infty} \frac{\varepsilon_s}{2}(-1)^s \left\{ I_{m-s}(\alpha\, r) + \chi^\zeta I_{-m-s}(\alpha\, r)\right\} \frac{\partial\, \mathcal{F}^{\phi\zeta}_{sn}(r)}{\partial\, r}, \tag{59d}$$

$$\mathbb{G}^{u\zeta}_{mn}(r) = \sum_{s=0}^{\infty} \frac{\varepsilon_s}{2}(-1)^s \left\{ I_{m-s}(\alpha\, r) + \chi^\zeta I_{-m-s}(\alpha\, r)\right\} \frac{\partial\, \mathcal{G}^{u\zeta}_{sn}(r)}{\partial\, r}, \tag{59e}$$

$$\mathbb{G}^{\phi\zeta}_{mn}(r) = \sum_{s=0}^{\infty} \frac{\varepsilon_s}{2}(-1)^s \left\{ I_{m-s}(\alpha\, r) + \chi^\zeta I_{-m-s}(\alpha\, r)\right\} \frac{\partial\, \mathcal{G}^{\phi\zeta}_{sn}(r)}{\partial\, r}. \tag{59f}$$

Subsequently, by employing Eqs. (6), (3), (33), (43), (44), (47), (56), (58) and the orthogonality conditions associated to $\sin(m\theta)$ and $\cos(m\theta)$, the following system of linear algebraic equations for the coefficients a^ζ_n, b^ζ_n, c^ζ_n, and d^ζ_n is inferred:

$$\sum_{n=0}^{\infty} \begin{bmatrix} \Lambda^{c(11)}_{mn} & \Lambda^{c(12)}_{mn} & \Lambda^{c(13)}_{mn} & \Lambda^{c(14)}_{mn} \\ \Lambda^{c(21)}_{mn} & \Lambda^{c(22)}_{mn} & \Lambda^{c(23)}_{mn} & \Lambda^{c(24)}_{mn} \\ \Lambda^{c(31)}_{mn} & \Lambda^{c(32)}_{mn} & \Lambda^{c(33)}_{mn} & \Lambda^{c(34)}_{mn} \\ \Lambda^{c(41)}_{mn} & \Lambda^{c(42)}_{mn} & \Lambda^{c(43)}_{mn} & \Lambda^{c(44)}_{mn} \end{bmatrix} \begin{bmatrix} a^c_n \\ b^c_n \\ c^c_n \\ d^c_n \end{bmatrix} = \begin{bmatrix} \Lambda^{c(1)}_{m} \\ \Lambda^{c(2)}_{m} \\ \Lambda^{c(3)}_{m} \\ \Lambda^{c(4)}_{m} \end{bmatrix}, \quad m = 0, 1, 2, \ldots, \tag{60a}$$

$$\sum_{n=1}^{\infty} \begin{bmatrix} \Lambda^{s(11)}_{mn} & \Lambda^{s(12)}_{mn} & \Lambda^{s(13)}_{mn} & \Lambda^{s(14)}_{mn} \\ \Lambda^{s(21)}_{mn} & \Lambda^{s(22)}_{mn} & \Lambda^{s(23)}_{mn} & \Lambda^{s(24)}_{mn} \\ \Lambda^{s(31)}_{mn} & \Lambda^{s(32)}_{mn} & \Lambda^{s(33)}_{mn} & \Lambda^{s(34)}_{mn} \\ \Lambda^{s(41)}_{mn} & \Lambda^{s(42)}_{mn} & \Lambda^{s(43)}_{mn} & \Lambda^{s(44)}_{mn} \end{bmatrix} \begin{bmatrix} a^s_n \\ b^s_n \\ c^s_n \\ d^s_n \end{bmatrix} = \begin{bmatrix} \Lambda^{s(1)}_{m} \\ \Lambda^{s(2)}_{m} \\ \Lambda^{s(3)}_{m} \\ \Lambda^{s(4)}_{m} \end{bmatrix}, \quad m = 1, 2, 3, \ldots, \tag{60b}$$

where

$$\begin{aligned}
&\Lambda^{\zeta(11)}_{mn} = e^{-\frac{\alpha}{2}h}(-1)^m \frac{\varepsilon_m}{2}\mathcal{F}^{u\zeta}_{mn}(a),\ \Lambda^{\zeta(12)}_{mn} = e^{-\frac{\alpha}{2}h}(-1)^m \frac{\varepsilon_m}{2}\mathcal{F}^{\phi\zeta}_{mn}(a),\ \Lambda^{\zeta(13)}_{mn} = -\delta_{mn}J_n(k_2 a),\ \Lambda^{\zeta(14)}_{mn} = 0,\\
&\Lambda^{\zeta(21)}_{mn} = e^{-\frac{\alpha}{2}h}(-1)^m \frac{\varepsilon_m}{2}\left\{\mathcal{G}^{u\zeta}_{mn}(a) + \frac{e^0_1}{\kappa^0_1}\mathcal{F}^{u\zeta}_{mn}(a)\right\},\ \Lambda^{\zeta(22)}_{mn} = e^{-\frac{\alpha}{2}h}(-1)^m \frac{\varepsilon_m}{2}\left\{\mathcal{G}^{\phi\zeta}_{mn}(a) + \frac{e^0_1}{\kappa^0_1}\mathcal{F}^{\phi\zeta}_{mn}(a)\right\},\\
&\Lambda^{\zeta(23)}_{mn} = -\delta_{mn}\frac{e_2}{\kappa_2}J_n(k_2 a),\ \Lambda^{\zeta(24)}_{mn} = -\delta_{mn}a^n,\\
&\Lambda^{\zeta(31)}_{mn} = e^{\frac{\alpha}{2}h}\frac{\varepsilon_m}{2}\left\{e^0_1\mathbb{G}^{u\zeta}_{mn}(a) + p^0_1\mathbb{F}^{u\zeta}_{mn}(a)\right\},\ \Lambda^{\zeta(32)}_{mn} = e^{\frac{\alpha}{2}h}\frac{\varepsilon_m}{2}\left\{e^0_1\mathbb{G}^{\phi\zeta}_{mn}(a) + p^0_1\mathbb{F}^{\phi\zeta}_{mn}(a)\right\},\\
&\Lambda^{\zeta(33)}_{mn} = -\delta_{mn}p_2 J'_n(k_2 a),\ \Lambda^{\zeta(34)}_{mn} = -\delta_{mn}e_2\, n\, a^{n-1},\\
&\Lambda^{\zeta(41)}_{mn} = -e^{\frac{\alpha}{2}h}\frac{\varepsilon_m}{2}\kappa^0_1\mathbb{G}^{u\zeta}_{mn}(a),\ \Lambda^{\zeta(42)}_{mn} = -e^{\frac{\alpha}{2}h}\frac{\varepsilon_m}{2}\kappa^0_1\mathbb{G}^{\phi\zeta}_{mn}(a),\ \Lambda^{\zeta(43)}_{mn} = 0,\ \Lambda^{\zeta(44)}_{mn} = \delta_{mn}\kappa_2\, n\, a^{n-1},\\
&\Lambda^{\zeta(1)}_{m} = -(-1)^m\frac{\varepsilon_m}{2}Q^\zeta_m(a),\ \Lambda^{\zeta(2)}_{m} = -(-1)^m\frac{\varepsilon_m}{2}\frac{e^0_1}{\kappa^0_1}\left\{Q^\zeta_m(a) - Z^\zeta_m(a)\right\},\\
&\Lambda^{\zeta(3)}_{m} = -e^{\alpha\, h}\frac{\varepsilon_m}{2}\left\{p^0_1\mathbb{Q}^\zeta_m(a) - \frac{{e^0_1}^2}{\kappa^0_1}\mathbb{Z}^\zeta_m(a)\right\},\ \Lambda^{\zeta(4)}_{m} = -e^{\alpha\, h}\frac{\varepsilon_m}{2}e^0_1\mathbb{Z}^\zeta_m(a).
\end{aligned} \tag{61}$$

4. Numerical results and discussion

Based on multipole expansion method, an analytical solution for the scattering problem of transverse surface waves by a homogeneous circular piezoelectric fiber surrounded by an exponentially graded piezoelectric half-space has been presented. In this section, several descriptive examples are provided to examine

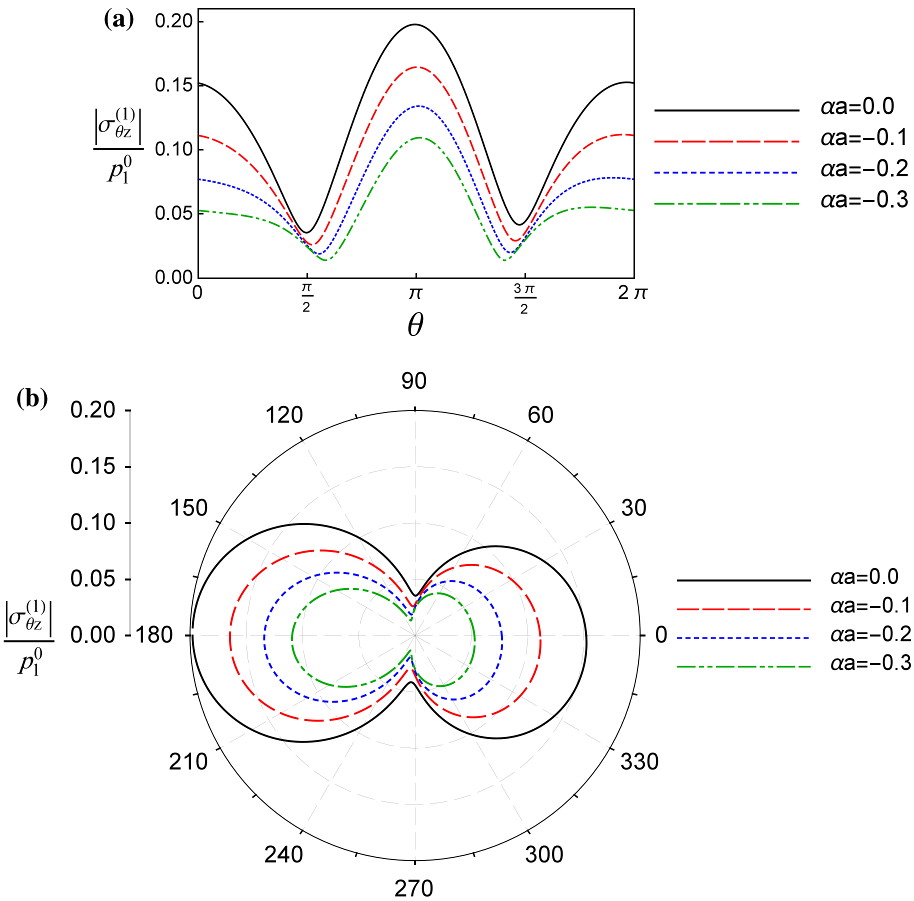

Fig. 3. **a** Distribution of the stress component $|\sigma_{\theta z}^{(1)}|/p_1^0$ along the FGPM substrate–fiber interface just inside the substrate for different values of the normalized gradient coefficient, αa. Part **b** represents the corresponding polar distribution

the dynamic response of the medium. In particular, we intend to examine the effects of the exponential coefficient, α the distance between the center of the fiber and the free surface of the half-space, b and the frequency, ω on the normalized absolute value of the stress component, $|\sigma_{\theta z}^{(1)}|/p_1^0$ along the fiber–substrate interface just inside the substrate. Utilizing Eqs. (6), (3), (7), (47), and (56) yields:

$$\sigma_{\theta z}^{\mathrm{i}(1)}(a,\theta) = \mu_1^0 e^{\alpha h}\frac{1}{a}\sum_{\zeta=c,s}\sum_{m=0}^{\infty}\frac{\varepsilon_m}{2}\bar{\mathbb{Q}}_m^{\zeta}(a)\bar{\mathcal{T}}_{\zeta}(m\theta)$$

$$+\frac{{e_1^0}^2}{\kappa_1^0}e^{\alpha h}\frac{1}{a}\sum_{\zeta=c,s}\sum_{m=0}^{\infty}\frac{\varepsilon_m}{2}\left\{\bar{\mathbb{Q}}_m^{\zeta}(a)-\bar{\mathbb{Z}}_m^{\zeta}(a)\right\}\bar{\mathcal{T}}_{\zeta}(m\theta), \tag{62a}$$

$$\sigma_{\theta z}^{\mathrm{s}(1)}(a,\theta) = \mu_1^0 e^{\frac{\alpha}{2}h}\sum_{\zeta=c,s}\sum_{n=0}^{\infty}\sum_{m=0}^{\infty}\frac{\varepsilon_m}{2}\left(a_n^{\zeta}\bar{\mathbb{F}}_{mn}^{u\zeta}(a)+b_n^{\zeta}\bar{\mathbb{F}}_{mn}^{\phi\zeta}(a)\right)\bar{\mathcal{T}}_{\zeta}(m\theta)$$

$$+e_1^0 e^{\frac{\alpha}{2}h}\sum_{\zeta=c,s}\sum_{n=0}^{\infty}\sum_{m=0}^{\infty}\frac{\varepsilon_m}{2}\left(a_n^{\zeta}\left\{\bar{\mathbb{G}}_{mn}^{u\zeta}(a)+\frac{e_1^0}{\kappa_1^0}\bar{\mathbb{F}}_{mn}^{u\zeta}(a)\right\}\right. \tag{62b}$$

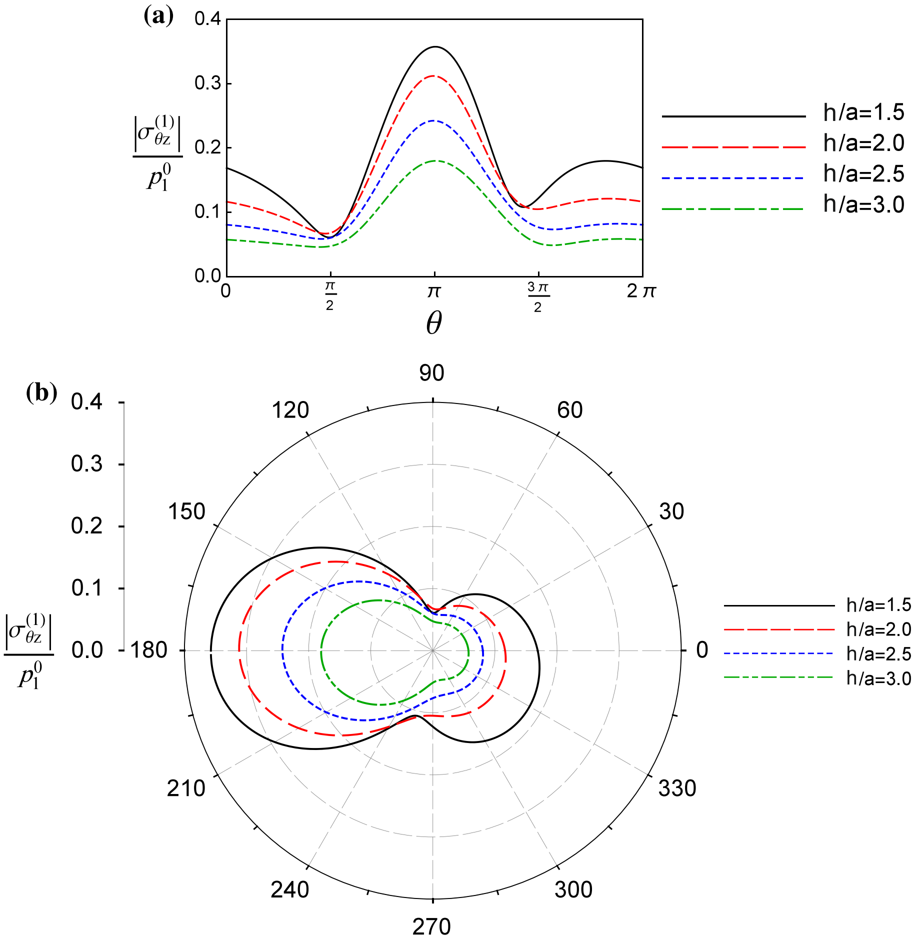

FIG. 4. **a** Distribution of the stress component $|\sigma_{\theta z}^{(1)}|/p_1^0$ along the FGPM substrate–fiber interface just inside the substrate for different values of the normalized distance between the center of the fiber and the free surface, h/a. Part **b** represents the corresponding polar distribution

$$+\,b_n^{\zeta}\left\{\bar{\mathbb{G}}_{mn}^{\phi\zeta}(a)+\frac{e_1^0}{\kappa_1^0}\bar{\mathbb{F}}_{mn}^{\phi\zeta}(a)\right\}\Bigg)\,\bar{\mathcal{T}}_{\zeta}(m\theta), \tag{62c}$$

in which $\bar{\mathcal{T}}_{\zeta}(m\theta)=\sin(m\theta)$ if $\zeta=c$ and $\bar{\mathcal{T}}_{\zeta}(m\theta)=\cos(m\theta)$ if $\zeta=s$ and

$$\bar{\mathbb{Q}}_m^{\zeta}(a)=-\sum_{s=0}^{\infty}\frac{\varepsilon_s}{2}(-1)^s\left\{I_{m-s}(\alpha\,a)+\chi^{\zeta}I_{-m-s}(\alpha\,a)\right\}(\chi^{\zeta}s)Q_s^{\zeta}(a), \tag{63a}$$

$$\bar{\mathbb{Z}}_m^{\zeta}(a)=-\sum_{s=0}^{\infty}\frac{\varepsilon_s}{2}(-1)^s\left\{I_{m-s}(\alpha\,a)+\chi^{\zeta}I_{-m-s}(\alpha\,a)\right\}(\chi^{\zeta}s)Z_s^{\zeta}(a), \tag{63b}$$

$$\bar{\mathbb{F}}_{mn}^{u\zeta}(a)=-\sum_{s=0}^{\infty}\frac{\varepsilon_s}{2}(-1)^s\left\{I_{m-s}(\alpha\,a)+\chi^{\zeta}I_{-m-s}(\alpha\,a)\right\}(\chi^{\zeta}s)\mathcal{F}_{sn}^{u\zeta}(a), \tag{63c}$$

$$\bar{\mathbb{F}}_{mn}^{\phi\zeta}(a)=-\sum_{s=0}^{\infty}\frac{\varepsilon_s}{2}(-1)^s\left\{I_{m-s}(\alpha\,a)+\chi^{\zeta}I_{-m-s}(\alpha\,a)\right\}(\chi^{\zeta}s)\mathcal{F}_{sn}^{\phi\zeta}(a), \tag{63d}$$

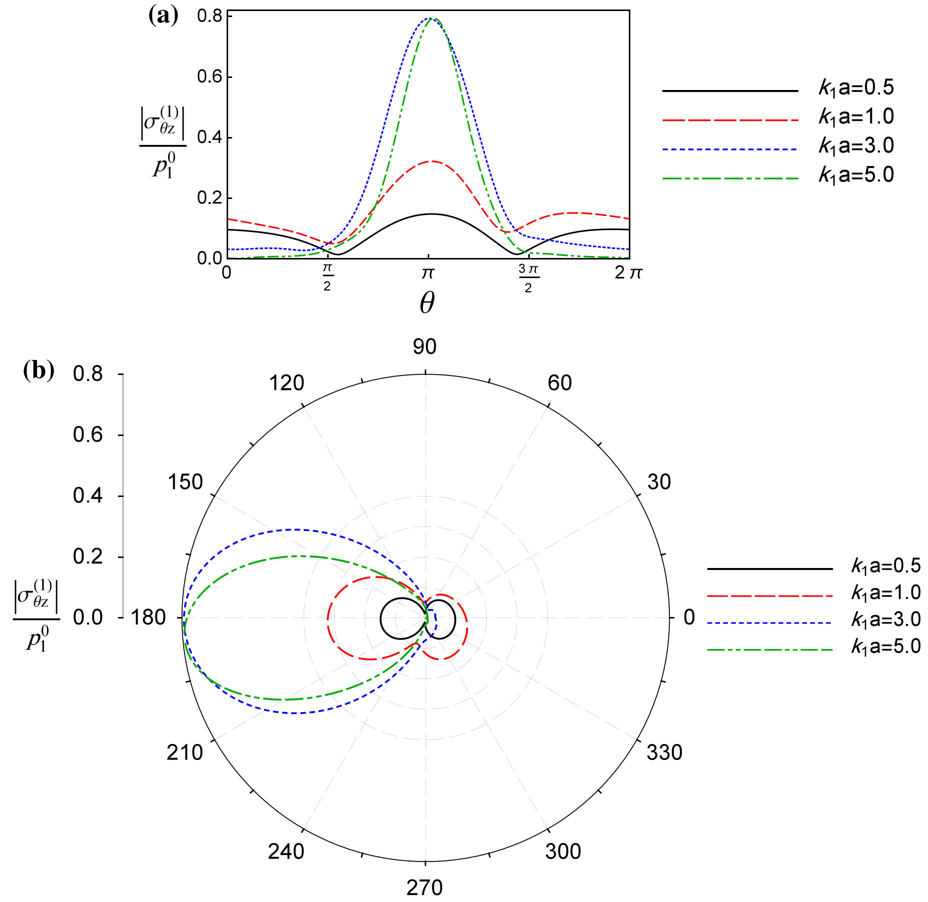

FIG. 5. **a** Distribution of the stress component $|\sigma_{\theta z}^{(1)}|/p_1^0$ along the FGPM substrate–fiber interface just inside the substrate for different values of the normalized wave number, k_1a. Part **b** represents the corresponding polar distribution

$$\bar{\mathbb{G}}_{mn}^{u\zeta}(a) = -\sum_{s=0}^{\infty} \frac{\varepsilon_s}{2}(-1)^s \left\{ I_{m-s}(\alpha\, a) + \chi^{\zeta} I_{-m-s}(\alpha\, a) \right\} (\chi^{\zeta} s) \mathcal{G}_{sn}^{u\zeta}(a), \tag{63e}$$

$$\bar{\mathbb{G}}_{mn}^{\phi\zeta}(a) = -\sum_{s=0}^{\infty} \frac{\varepsilon_s}{2}(-1)^s \left\{ I_{m-s}(\alpha\, a) + \chi^{\zeta} I_{-m-s}(\alpha\, a) \right\} (\chi^{\zeta} s) \mathcal{G}_{sn}^{\phi\zeta}(a). \tag{63f}$$

In all the examples given in this section, it is assumed that the piezoelectric fiber is made of $BaTiO_3$ with electromechanical properties: $\mu_2 = 43 \times 10^9$ N m^{-2}; $e_2 = 11.6$ C m^{-2}; $\kappa_2 = 112 \times 10^{-10}$ F m^{-1}; $\rho_2 = 5.7 \times 10^3$ kg m^{-3}. Moreover, the electromechanical material properties of the exponentially graded half-space at the free surface are: $\mu_1^0 = 25.6 \times 10^9$ N m^{-2}; $e_1^0 = 12.7$ C m^{-2}; $\kappa_1^0 = 64.64 \times 10^{-10}$ F m^{-1}; $\rho_1^0 = 7.5 \times 10^3$ kg m^{-3}. The frequency, the distance of the center of the fiber to the surface of the substrate, and the exponential coefficient are normalized as $\omega a/c_{\mathrm{sh}}^{(1)}$, and αa, respectively.

In order to assess the influence of the dimensionless exponential coefficient, αa on the distribution of the normalized stress component, $|\sigma_{\theta z}^{(1)}|/p_1^0$ along the FGP substrate–fiber interface just inside the substrate, we keep $\omega a/c_{\mathrm{sh}}^{(1)} = 0.5$ and $b/a = 2$ fixed. Then, the distributions of $|\sigma_{\theta z}^{(1)}|/p_1^0$ for different values of $\alpha a = 0, -0.1, -0.2, -0.3$ are plotted in Fig. 3a and b; Fig. 3b represents the polar plot. It is observed that, the gradient coefficient, αa has significant effect on the stress distribution. As it can be seen, $|\sigma_{\theta z}^{(1)}|$ increases as absolute value of the gradient coefficient decreases.

Next, to examine the effect of the distance between the center of the piezoelectric fiber and the free surface of the FGP half-space, we hold $\omega a/c_{\rm sh}^{(1)} = 1$ and $\alpha a = -0.1$ fixed. Subsequently, for various values of $b/a = 1.5, 2, 2.5$, and 3 the corresponding distributions of $|\sigma_{\theta z}^{(1)}|/p_1^0$ along the FGP substrate–fiber interface are plotted in Fig. 4a and b. From the polar distributions of $|\sigma_{\theta z}^{(1)}|/p_1^0$ shown in Fig. 4b, it is clearly seen that as the fiber is located closer to the free surface it experiences larger absolute stress value, and the associated stress distribution is skewed. While at larger distances where the surface effect diminishes, the distribution becomes nearly symmetrical.

To assess the effect of the frequency on the absolute value of the stress component, $|\sigma_{\theta z}^{(1)}|/p_1^0$ along the boundary of the piezoelectric fiber with its center at a depth of $b/a = 1.5$ beneath the free surface, we keep $\alpha a = -0.25$ fixed. Then, for different values of $\omega a/c_{\rm sh}^{(1)} = 0.5, 1, 3$, and 5 the corresponding distributions of the normalized magnitude of the stress component, $|\sigma_{\theta z}^{(1)}|/p_1^0$ along the fiber–substrate interface just inside the substrate are calculated and plotted in Fig. 5a and b. It can be observed that, the frequency of the propagating transverse surface waves has significant effect on the stress distribution.

5. Conclusion

Scattering of transverse surface waves by a circular piezoelectric fiber which is embedded near the free surface of a FGPM half-space with exponentially varying electromechanical properties is addressed using multipole expansion method. The scattered displacement and electric potential fields are expressed as series expansion in terms of multipole functions which satisfy: (a) the electromechanical field equations in the substrate, (b) the free traction and electrically short conditions along the free surface of the substrate, and (c) the radiation conditions at infinity. The simple poles of these multipole functions are related to the roots of the pertinent dispersion relation. By satisfying some appropriate boundary conditions peculiar to the problem of interest, the analytical expressions for the pertinent electromechanical fields are derived. In the section on the descriptive examples, the effects of several parameters on the scattered stress field have been examined. It is realized that the inhomogeneity coefficient, the frequency of the incident transverse surface waves, and the distance between the center of the fiber and the substrate's free surface have significant effect on the dynamic response of the medium.

Acknowledgements

This research was in part supported under Grant G950915 from the office of the Innovative Research and Technological Developments at Sharif University of Technology.

References

[1] Jakoby, B., Vellekoop, M.J.: Properties of love waves: applications in sensors. Smart Mater. struct. **6**(6), 668 (1997)
[2] Majorkowska-Knap, K., Lenz, J.: Piezoelectric love waves in non-classical elastic dielectrics. Int. J. Eng. Sci. **27**(8), 879–893 (1989)
[3] Qian, Z.H., Jin, F., Lu, T., Kishimoto, K.: Transverse surface waves in functionally graded piezoelectric materials with exponential variation. Smart Mater. Struct. **17**(6), 065005 (2008)
[4] Du, J., Jin, X., Wang, J., Xian, K.: Love wave propagation in functionally graded piezoelectric material layer. Ultrasonics **46**, 13–22 (2007)

[5] Qian, Z., Jin, F., Wang, Z., Kishimoto, K.: Transverse surface waves on a piezoelectric material carrying a functionally graded layer of finite thickness. Int. J. Eng. Sci. **45**, 455–66 (2007)
[6] Eskandari, M., Shodja, H.M.: Love waves propagation in functionally graded piezoelectric material with quadratic variation. J. Sounds Vib. **313**, 195–204 (2008)
[7] Shodja, H.M., Eskandari, S., Eskandari, M.: Shear horizontal surface acoustic waves in functionally graded magneto-electro-elastic half-space. J. Eng. Math. **97**(1), 83–100 (2016)
[8] Fang, X.Q., Hu, C., Huang, W.H.: Dynamic stress of a circular cavity buried in a semi-infinite functionally graded piezoelectric material subjected to shear waves. Eur. J. Mech. A Solids **26**(6), 1016–1028 (2007)
[9] Fang, X.Q., Liu, J.X., Wang, X.H., Zhang, L.L.: Dynamic stress around two holes buried in a functionally graded piezoelectric material layer under electro-elastic waves. Philos. Mag. Lett. **90**(5), 361–380 (2010)
[10] Martin, P.A.: Scattering by a cavity in an exponentially graded half-space. J. Appl. Mech. **76**, 031009 (2009). 4 pages
[11] Ghafarollahi, A., Shodja, H.M.: Scattering of SH-waves by a nano-fiber beneath the interface of two bonded half-spaces within surface/interface elasticity via multipole expansion. Int. J. Solids Struct. **130**, 258–279 (2018)
[12] Ghafarollahi, A., Shodja, H.M.: Scattering of SH-waves by an elliptic cavity/crack beneath the interface between functionally graded and homogeneous half-spaces via multipole expansion method. J. Sound Vib. **435**, 372–389 (2018)
[13] Lamb, H.: On the propagation of tremors over the surface of an elastic solid. In: Philosophical Transactions of the Royal Society of London. Series A, Containing Papers of a Mathematical or Physical Character, vol 203, pp. 1–42 (1904)

A. Ghafarollahi
Laboratory for Multiscale Mechanics Modeling
EPFL
1015 Lausanne
Switzerland
e-mail: alireza.ghafarollahi@epfl.ch

H. M. Shodja
Department of Civil Engineering
Sharif University of Technology
Tehran
Iran
e-mail: shodja@sharif.edu

(Received: August 23, 2018; revised: March 18, 2019)